PROCEEDINGS OF SCIENCE

Studies of photon production in association with jets at the ATLAS detector

Mark Stockton[*†]
University of Oregon (USA), CERN (Switzerland)
E-mail: mark.stockton@cern.ch

The production of prompt photons in association with jets in proton-proton collisions at the LHC provides a testing ground for perturbative QCD (pQCD) with a hard colourless probe less affected by hadronisation effects than jet production. The measurements of the angular correlations between the photon and the jets can be used to probe the dynamics of the hard-scattering process. We present here the latest ATLAS cross-section measurement of isolated photon plus jet at $\sqrt{s} = 13$ TeV, differential in a wide range of kinematic variables describing the photon plus jet production dynamic. We will also present for the first time ATLAS measurements on the differential cross sections of isolated-photon plus heavy-flavour jet production at $\sqrt{s} = 8$ TeV. The results are compared to recent theoretical predictions.

XXVI International Workshop on Deep-Inelastic Scattering and Related Subjects (DIS2018)
16-20 April 2018
Kobe, Japan

[*]Speaker.
[†]On behalf of the ATLAS Collaboration.

PoS(DIS2018)004

1. Introduction

The results presented in this paper focus on prompt photons, i.e. photons that do not originate from hadronic decays. Prompt photons are produced by the direct and fragmentation processes. At leading order (LO) these processes are well separated, and are characterised by the spin of the exchange particle which results in different angular distributions between the photon and jet.

The results presented here focus on photon plus jet production at $\sqrt{s} = 13$ TeV [1] and the measurement of photon plus heavy flavour jet production at $\sqrt{s} = 8$ TeV [2]. The LHC pp collision data recorded by the ATLAS experiment [3] at $\sqrt{s} = 8$ TeV were recorded in 2012 and corresponds to 20.3fb^{-1} with an average of 20.7 interactions per crossing (otherwise referred to as pileup), whereas the $\sqrt{s} = 13$ TeV data were recorded in 2015 and corresponds to 3.2fb^{-1} with lower pileup of 13.7. At previous DIS meetings earlier ATLAS photon plus jet measurements have been shown, at $\sqrt{s} = 7$ TeV [4, 5] and at $\sqrt{s} = 8$ TeV [6].

Photons are selected in ATLAS [7, 8] in the regions $|\eta| < 1.37$ (central) and $1.56 < |\eta| < 2.37$ (forward). To remove hadron and τ background identification requirements are applied to the lateral and longitudinal energy profiles of the shower in the calorimeter. Further calorimeter isolation is applied where the energy around the photon (E_T^{iso}) must satisfy: $E_T^{iso} < 0.0042 \times E_T^{\gamma} + 4.8$ GeV where this scales with the photon energy (E_T^{γ}) and is also corrected for pileup using jet area method [9, 10]. As in the other ATLAS photon cross section measurements a 2D-sidebands technique [11] is used to subtract the remaining background, which separates the photon candidates based on whether they pass or fail both/either the photon isolation and/or identification criteria. This is data driven, but uses simulation to estimate signal contamination in the control regions. Finally the small electron background is removed using simulation (but is checked in data).

2. Photon plus jet

The photon plus jet measurement at $\sqrt{s} = 13$ TeV [1] uses the anti-k_T algorithm with a radius parameter of 0.4. The jets are built using topological clusters and then a multi-step calibration [12] procedure is applied. The leading jet is used in the analysis and must satisfy $p_T^{jet} > 100$ GeV and $y^{jet} < 2.37$. To distinguish the photon isolation cone and the jet they must be separated by $\Delta R > 0.8$. These jet selection criteria are used with photons with $E_T^{\gamma} > 125$ GeV to measure the cross sections as a function of E_T^{γ}, $p_T^{jet-lead}$ and $\Delta\phi^{\gamma-jet}$. For the measurements of $m^{\gamma-jet}$ and $|cos\theta^*|$ additional constraints ($|\eta^{\gamma} + y^{jet-lead}| < 2.37$, $|cos\theta^*| < 0.83$ and $m^{\gamma-jet} > 450$ GeV) are applied to remove bias due to the selection requirements on the photon and jet. Many sources of systematic uncertainty are estimated, but it is found that three dominate the measurement: the jet and photon energy scales and the photon identification. In each case the results are propagated through all steps of the analysis to keep correlations.

The fiducial measured cross section is: $\sigma_{meas} = 300 \pm 10(exp.) \pm 6(lumi.)$ pb. This is consistent with next-to-leading order (NLO) theory (both JetPhox and NLO Sherpa). In the differential results compared to LO predictions there is a very good agreement in all variables for LO Sherpa and Pythia, except for Pythia in the measurement of $p_T^{jet-lead}$, as shown in figure 1. The differential measurement in $|cos\theta^*|$, also shown in figure 1, illustrates the contributions of the two processes for production of prompt photons. Comparing to NLO, the differential results show a good agree-

ment over six orders of magnitude in E_T^γ, as shown in figure 2, and both predictions are within the experimental uncertainties. NLO Sherpa includes the processes $\gamma+1/2\,jet$ at NLO and $\gamma+3/4\,jet$ at LO in addition to its parton shower, so it is able to reproduce data to $\pi/2$ in $\Delta\phi^{\gamma-jet}$, also shown in figure 2. The JetPhox (NLO Sherpa) predictions use the MMHT2014 (NNPDF3.0) PDF sets, but no PDF set dependence is observed as using alternative sets (including CT14) results in differences smaller than 5%. Overall the results show good agreement of pQCD in photon jet dynamics at 13 TeV.

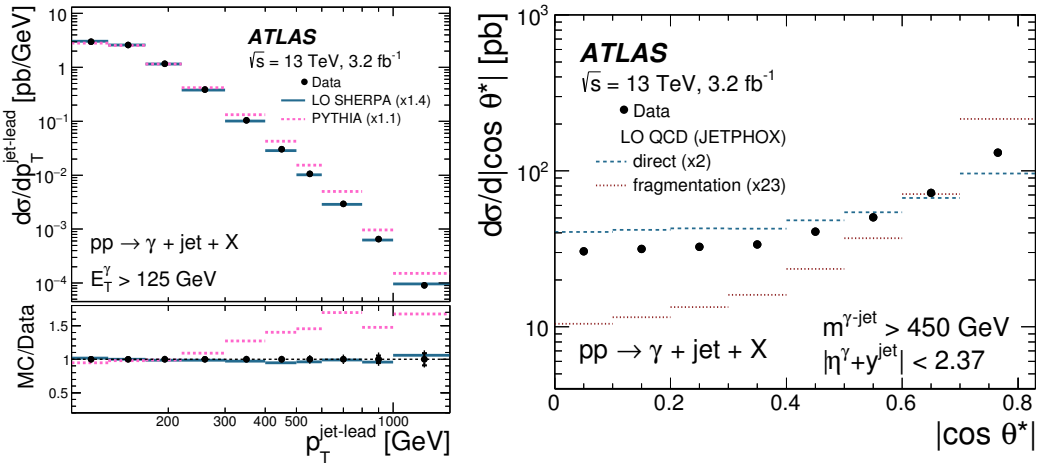

Figure 1: Measured cross sections [1] for isolated-photon plus jet production (dots) as a function of $p_T^{jet-lead}$ and $|cos\theta^*|$. (Left) The predictions from LO Sherpa (solid lines) and Pythia (dashed lines) are normalised to the integrated measured cross sections (using the factors indicated in parentheses). (Right) The LO QCD predictions from JetPhox for the direct (dashed lines) and fragmentation (dotted lines) processes are shown separately and are normalised to the integrated measured cross section by the factors shown in parentheses.

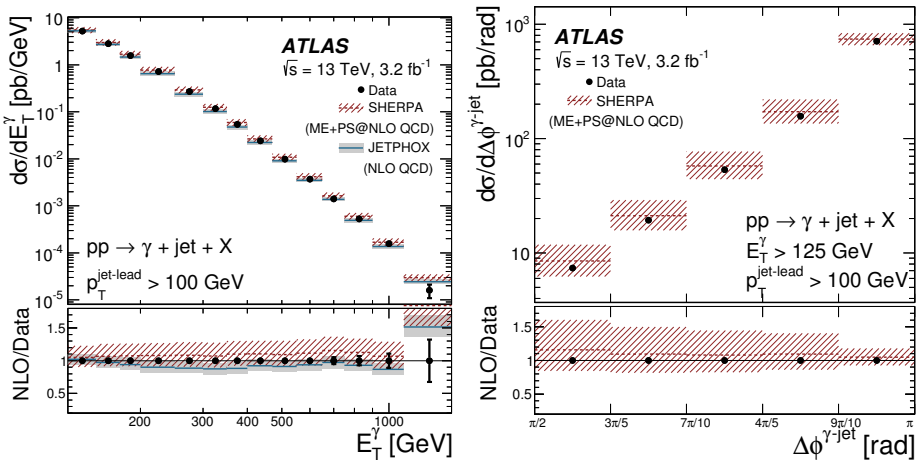

Figure 2: Measured cross sections [1] for isolated-photon plus jet production (dots) as functions of E_T^γ and $\Delta\phi^{\gamma-jet}$. The NLO QCD plus parton shower predictions from NLO Sherpa (dashed lines) and the NLO QCD predictions from Jetphox corrected for hadronisation and UE effects (solid lines) are also shown.

3. Photon plus heavy flavour jet

The photon plus heavy flavour jet measurement at $\sqrt{s} = 8$ TeV [2] follows a very similar selection to the photon plus jet measurement above, but probes lower energy. The photon is now selected for $E_T^\gamma > 25$ GeV, which requires using prescaled triggers, and the jet similarly must now satisfy $p_T^{jet} > 20$ GeV, which requires further suppression of pileup jets for jets with $p_T^{jet} < 50$ GeV. The main difference from the measurements comes from the addition of the requirement on jet flavour. This uses the MV1c (neural network) algorithm [13], which is trained to specifically identify b-jets with enhanced rejection of c-jets. It uses discriminants from three other algorithms based on different aspects of jet tracking information from secondary vertices. In the measurement a maximum likelihood template fit is performed in bins based on tagger efficiency selections. From this the γ+b and γ+c contributions are extracted simultaneously for ranges of E_T^γ. The extracted contributions, and an example of the template fit distribution, are shown in figure 3. The calibration of the tagger discriminant is found to be the largest uncertainty on the measurement, along with the finite number of data statistics in the highest and lowest E_T^γ bins. The uncertainties are larger for the γ+c measurement and the forward region has larger uncertainties for both measurements.

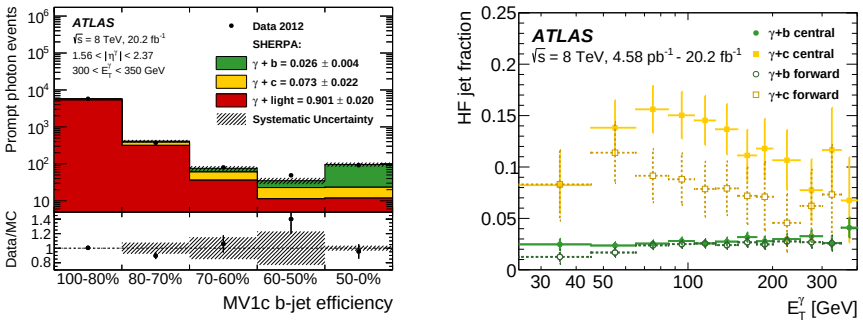

Figure 3: (Left [2]) Example of a template fit to the MV1c tagger discriminant distribution used to measure the γ+b and γ+c fractions. The data yield is shown after subtraction of background photons. The numbers in the legend are the fractions of each template after the fit and their statistical uncertainties. (Right [2]) The heavy-flavour jet fractions obtained from the template fits as a function of E_T^γ. The fractions are relative to the yield of selected photon plus jet data events after subtraction of background photons.

The fiducial cross sections, shown in figure 4, present an overall good agreement of the calculations in all measurements. At LO, Sherpa is found to performs well in all measurements, whereas above 150 GeV Pythia is found to underestimate the data in the γ+b measurement. Both the 4 and 5 flavour schemes are tested when using MadGraph and they both agree at low E_T^γ in γ+b, but the 5 flavour scheme performs better for the region $125 < E_T^\gamma < 200$ GeV. Above this, gluon splitting is important and the resulting disagreement between the predictions and the measurement shows the need for higher order calculations. Good agreement is seen across the whole of the γ+c measurement, as gluon splitting is less important for the E_T^γ range measured. This measurement is sensitive to the intrinsic charm hypothesis [14] and predictions are made using PDF sets with varying sizes of this contribution: BHPS1 (0.6%), BHPS2 (2.1%), NNPDF FittedC (0.26%). All of these PDF sets predict higher cross sections in the forward region, as expected, with BHPS2 deviating the most. The ratios between the central and forward regions in figure 5 show the above features clearly.

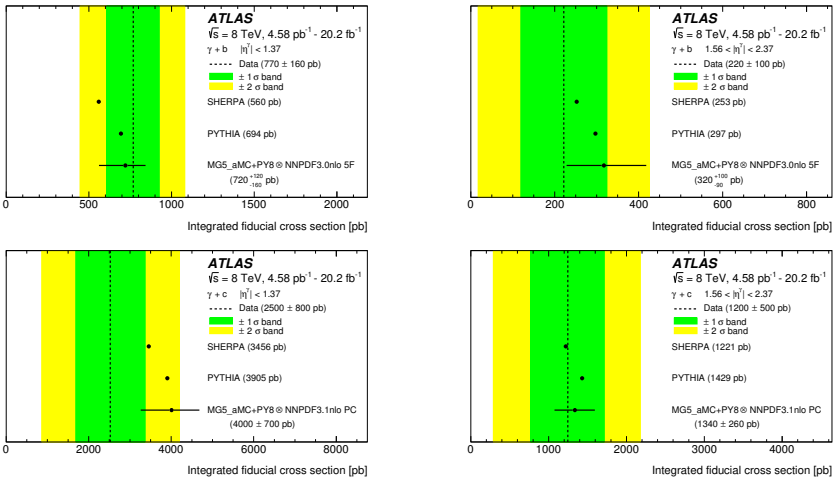

Figure 4: Measured integrated γ+b and γ+c cross sections [2] compared to theoretical predictions, in the central and forward regions. The MG5_aMC+PY8 label refers to the MadGraph5_aMC NLO calculations interfaced to PYTHIA. The 5F label refers to the PDF set using the 5 flavour scheme and the PC label refers to the perturbative charm PDF set. No uncertainty is provided for the LO predictions.

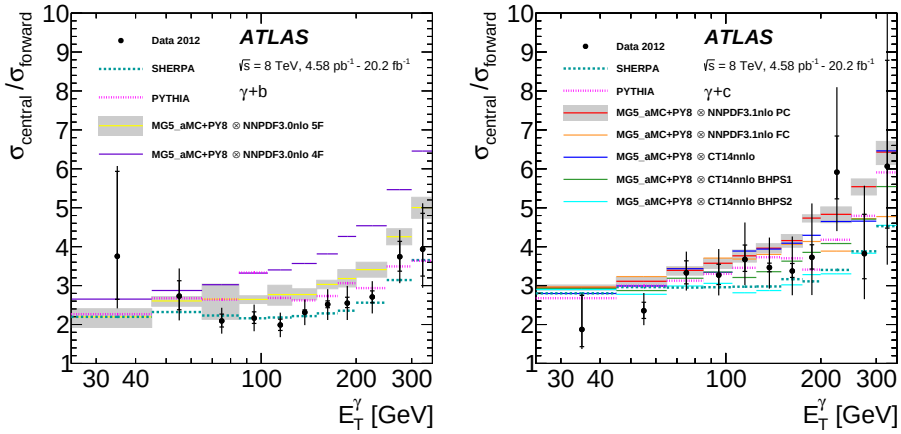

Figure 5: Cross-section ratios of the central region to the forward region [2], for (left) γ+b and (right) γ+c. The statistical uncertainty is represented as horizontal marks on the error bars of the data points, while the total measurement uncertainty is represented by the complete length of the error bars. The MG5_aMC+PY8 label in the legend refers to the MadGraph5_aMC@NLO calculations interfaced to PYTHIA. The 5F and 4F labels in the legend refer to PDF sets with 5 (used for all the predictions for γ+c) and 4 flavours respectively. The PC and FC labels in the legend refer to perturbative charm and fitted charm PDF sets respectively. The theoretical uncertainty in the MadGraph5_aMC@NLO predictions is displayed for a single PDF set since it is similar for each of the PDF sets.

4. Summary

The existing ATLAS photon plus jet measurements have been built upon. Firstly by extending to 13 TeV, where LO predictions performs well in all measurements (apart from Pythia in $p_T^{jet-lead}$) and the measured cross sections are consistent with NLO pQCD predictions. Secondly the first measurement of photon plus heavy flavour at the LHC is performed. For γ+b the best de-

scription is provided by Sherpa, but the NLO predictions underestimate the data with the 5 flavour scheme working better than that of the 4 flavour scheme. The γ+c measurement has larger experimental uncertainties and all predictions are found to be in agreement with data, where the PDF sets with/without intrinsic charm included give deviations similar to the measurement uncertainties. It will be exciting to see these results performed with improved theory calculations and the increased LHC pp collision data recorded by ATLAS.

References

[1] ATLAS collaboration, *Measurement of the cross section for inclusive isolated-photon production in pp collisions at $\sqrt{s} = 13$ TeV using the ATLAS detector*, *Phys. Lett.* **B770** (2017) 473 [1701.06882].

[2] ATLAS collaboration, *Measurement of differential cross sections of isolated-photon plus heavy-flavour jet production in pp collisions at $\sqrt{s} = 8$ TeV using the ATLAS detector*, *Phys. Lett.* **B776** (2018) 295 [1710.09560].

[3] ATLAS collaboration, *The ATLAS Experiment at the CERN Large Hadron Collider*, *JINST* **3** (2008) S08003.

[4] ATLAS collaboration, *Measurement of the production cross section of an isolated photon associated with jets in proton-proton collisions at $\sqrt{s} = 7$ TeV with the ATLAS detector*, *Phys. Rev.* **D85** (2012) 092014 [1203.3161].

[5] ATLAS collaboration, *Dynamics of isolated-photon plus jet production in pp collisions at $\sqrt{(s)} = 7$ TeV with the ATLAS detector*, *Nucl. Phys.* **B875** (2013) 483 [1307.6795].

[6] ATLAS collaboration, *High-E_{T} isolated-photon plus jets production in pp collisions at $\sqrt{s} = 8$ TeV with the ATLAS detector*, *Nucl. Phys.* **B918** (2017) 257 [1611.06586].

[7] ATLAS collaboration, *Electron and photon energy calibration with the ATLAS detector using LHC Run 1 data*, *Eur. Phys. J.* **C74** (2014) 3071 [1407.5063].

[8] ATLAS collaboration, *Measurement of the photon identification efficiencies with the ATLAS detector using LHC Run-1 data*, *Eur. Phys. J.* **C76** (2016) 666 [1606.01813].

[9] M. Cacciari, G. P. Salam and G. Soyez, *The Catchment Area of Jets*, *JHEP* **04** (2008) 005 [0802.1188].

[10] M. Cacciari, G. P. Salam and S. Sapeta, *On the characterisation of the underlying event*, *JHEP* **04** (2010) 065 [0912.4926].

[11] ATLAS collaboration, *Measurement of the inclusive isolated prompt photon cross section in pp collisions at $\sqrt{s} = 7$ TeV with the ATLAS detector*, *Phys. Rev.* **D83** (2011) 052005 [1012.4389].

[12] ATLAS collaboration, *Jet energy scale measurements and their systematic uncertainties in proton-proton collisions at $\sqrt{s} = 13$ TeV with the ATLAS detector*, *Phys. Rev.* **D96** (2017) 072002 [1703.09665].

[13] ATLAS collaboration, *Performance of b-Jet Identification in the ATLAS Experiment*, *JINST* **11** (2016) P04008 [1512.01094].

[14] V. A. Bednyakov, M. A. Demichev, G. I. Lykasov, T. Stavreva and M. Stockton, *Searching for intrinsic charm in the proton at the LHC*, *Phys. Lett.* **B728** (2014) 602 [1305.3548].